Constraining work fluctuations of non-Hermitian dynamics across the exceptional point of a superconducting qubit

Serra Erdamar, ^{1,2} Maryam Abbasi, ² Byung Ha, ² Weijian Chen, ² Jacob Muldoon, ³ Yogesh Joglekar, ³ and Kater W. Murch ²

¹Department of Electrical and Systems Engineering, Washington University, St. Louis, Missouri 63130, USA

²Department of Physics, Washington University, St. Louis, Missouri 63130, USA

³Department of Physics, Indiana University-Purdue University Indianapolis, Indianapolis, Indiana 46202, USA



(Received 3 October 2023; revised 6 February 2024; accepted 21 March 2024; published 16 April 2024)

Thermodynamics constrains changes to the energy of a system, both deliberate and random, via its first and second laws. When the system is not in equilibrium, fluctuation theorems such as the Jarzynski equality further restrict the distributions of deliberate work done. Such fluctuation theorems have been experimentally verified in small, nonequilibrium quantum systems undergoing unitary or decohering dynamics. Yet, their validity in systems governed by a non-Hermitian Hamiltonian has long been contentious due to the false premise of the Hamiltonian's dual and equivalent roles in dynamics and energetics. Here we show that work fluctuations in a non-Hermitian qubit obey the Jarzynski equality even if its Hamiltonian has complex or purely imaginary eigenvalues. With postselection on a dissipative superconducting circuit undergoing a cyclic parameter sweep, we experimentally quantify the work distribution using projective energy measurements and show that the fate of the Jarzynski equality is determined by the parity-time symmetry of, and the energetics that result from, the corresponding non-Hermitian, Floquet Hamiltonian. By distinguishing the energetics from non-Hermitian dynamics, our results provide the recipe for investigating the nonequilibrium quantum thermodynamics of such open systems.

DOI: 10.1103/PhysRevResearch.6.L022013

I. INTRODUCTION

The concept of a small system coupled to a large reservoir is elemental to both thermodynamics and open quantum systems. In thermodynamics, a reservoir allows one to distinguish between two types of energetics: heat Q, the random energy transferred to the system from the reservoir, and work W, deliberately imparted to the system. The energy U of the system is additively changed by the two, thereby encoding the first law of quantum thermodynamics, $\Delta U = Q + W$ (Fig. 1, right inset) [1–6]. Conversely, a closed quantum system is governed by a Hermitian Hamiltonian H(t), undergoes unitary evolution with zero heat exchange, and its energy is equal to the expectation value of the generator of its dynamics H(t). When coupled to a reservoir, one describes its evolution by averaging over possible, consistent microstates of the reservoir. This averaging leads to (engineered) decoherence and dissipation [7]; the resulting dynamics are described by a Lindblad equation $\partial_t \rho = \mathcal{L} \rho$ for the reduced density matrix $\rho(t)$ of the system [8]. Here, the system-reservoir coupling results in trajectory-dependent heat and work that, when added together, gives a trajectory-independent change in the energy of the system [9]. In such cases, the internal energy operator H(t), which encodes the energy $U(t) \equiv \text{Tr}[\rho(t)H(t)]$, is distinct from the generator \mathcal{L} of its temporal dynamics.

Published by the American Physical Society under the terms of the Creative Commons Attribution 4.0 International license. Further distribution of this work must maintain attribution to the author(s) and the published article's title, journal citation, and DOI.

In addition to the work-energy theorem, work fluctuations of a nonequilibrium system with internal energy operator H(t) are further constrained by the Jarzynski equality [10–13]:

$$\langle e^{-\beta W} \rangle = \frac{Z(\tau)}{Z(0)} \equiv e^{-\beta \Delta F}.$$
 (1)

Here $\langle \cdot \rangle$ denotes trajectory-ensemble average, β^{-1} is the reservoir temperature, $Z(t) \equiv \operatorname{Tr} \exp[-\beta H(t)]$ is the system partition function, and $\Delta F \equiv F(\tau) - F(0)$ is the Helmholtz free energy change in time τ . The equality (1) supersedes the Jensen inequality $\Delta F \leqslant \langle W \rangle$ that constrains the amount of work done on a system and its free-energy change. In a quantum system with indefinite energy, a two-point-measurement (TPM) protocol quantifies changes in a system's energy ΔU [14,15] in terms of transition probabilities between energy eigenstates of the internal energy operator H(t) (Fig. 1). It entails performing a pair of projective measurements in the energy basis to quantify ΔU . These transition probabilities differ for unitary and Lindblad evolution and yet the Jarzynski equality (1) holds [16] for unital quantum maps [17,18], as has been experimentally verified [19–23].

In recent years, a third model of quantum dynamics obtained by postselecting on quantum trajectories with no quantum jumps has emerged [24,25]. With a non-Hermitian generator $H_{\rm eff}(t)=H(t)+i\Gamma(t)$ and a nonlinear, tracepreserving equation of motion [26], it maps pure states into pure states but changes the entropy of mixed states [27], thereby commingling salient features of unitary and Lindblad evolution. These non-Hermitian systems occur by considering a subspace of the larger dissipative system which is governed by Lindblad evolution. When the non-Hermitian $H_{\rm eff}$ has a

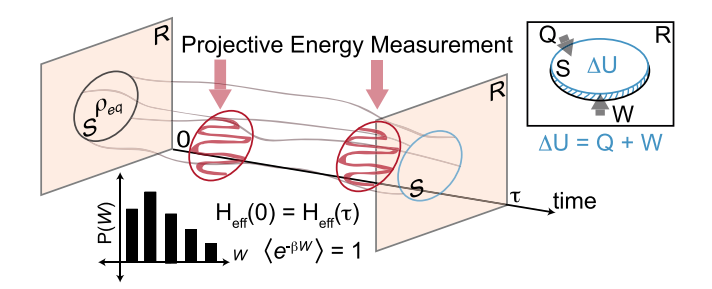


FIG. 1. Thermodynamics of open quantum systems. The first law of thermodynamics (right inset) states that the internal energy of a system (S) coupled to a reservoir (R) is additively changed by the heat Q and the work W. The generalized second law or the Jarzynski equality (1) governs the trajectory-dependent work fluctuations. For a quantum system starting in an equilibrium density matrix $\rho_{\rm eq}$, these work fluctuations are characterized by projective energy measurements leading to a discrete work distribution P(W). We show that for cyclic parameter variations in $H_{\rm eff}(t)$, the average exponentiated work is unity when the corresponding Floquet Hamiltonian $H_{\rm eff}^F$ has a parity-time symmetry, and its Floquet energy operator matches the system's initial energy operator.

real spectrum, its role in dynamics has been conflated with energetics, leading to predicted violations of the Jarzynski equality and Crooks fluctuation theorem when the spectrum of $H_{\rm eff}$ turns complex [28–33]. Fundamentally, the coherent, nonunitary, nonunital dynamics generated by $H_{\rm eff}$ begs the question: What are the constraints on quantum work fluctuations in such dynamics?

Here, we demonstrate the Jarzynski equality in a non-Hermitian qubit undergoing real-time parameter changes, including cases where $H_{\rm eff}(t)$ has complex eigenvalues at all times. For simplicity, we focus on cyclic parameter changes, where $H_{\rm eff}(0)=H_{\rm eff}(\tau)$; the final and initial partition functions are equal, thus $Z(\tau)/Z(0)=1$. For these cyclic parameter sweeps, the qubit dynamics is characterized by the nonunitary $G(\tau)=\mathbb{T}\exp[-i\int_0^\tau H_{\rm eff}(t')dt']\equiv \exp(-i\tau H_{\rm eff}^F)$ that defines the non-Hermitian Floquet Hamiltonian $H_{\rm eff}^F\equiv H^F+i\Gamma^F$, where H^F is the Floquet internal energy operator. We show that the Jarzynski equality $\langle e^{-\beta W}\rangle=1$ is satisfied when $H_{\rm eff}^F$ has an explicit or emergent parity-time (\mathcal{PT}) symmetry that guarantees real or complex-conjugate eigenvalues, and $H^F\propto H(0)$, i.e., the two internal energy operators have the same eigenbasis (see Appendix A).

II. NON-HERMITIAN DYNAMICS FROM NO-JUMP QUANTUM EVOLUTION

Our experimental platform comprises a superconducting transmon circuit with energy eigenstates labeled $\{|g\rangle, |e\rangle, |f\rangle\}$ dispersively coupled to a microwave cavity (see Sec. IV for more details). Bath engineering allows us to tune the radiative decay rates such that the spontaneous emission decay rate $\gamma_e = 1.57~\mu s^{-1}$ of state $|e\rangle$ by quantum jumps $|e\rangle \rightarrow |g\rangle$ is much larger than the decay rate $\gamma_f = 0.21~\mu s^{-1}$ from $|f\rangle \rightarrow |e\rangle$, leading to a decay contrast $\gamma \equiv \gamma_e - \gamma_f \approx \gamma_e$. The spontaneous emission dissipation operator associated with this decay is given by $L = \sqrt{\gamma} \sigma_- \equiv \sqrt{\gamma} |g\rangle \langle e|$. We postselect quantum trajectories with no quantum jumps to the $|g\rangle$ state,

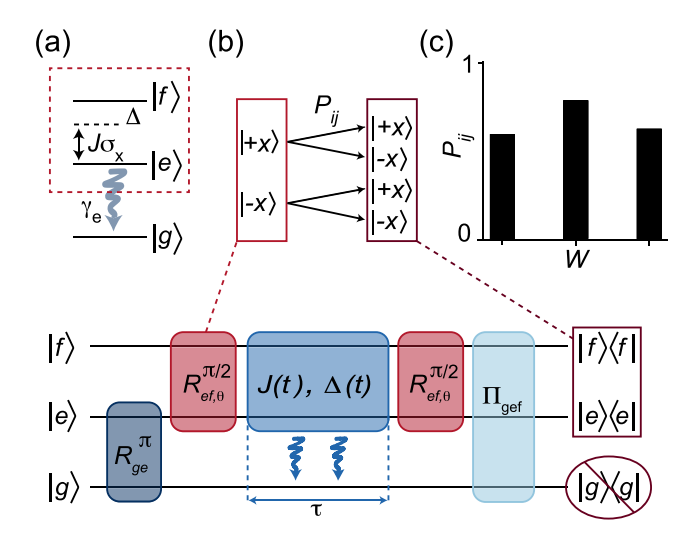


FIG. 2. Experimental setup. (a) A non-Hermitian qubit is realized as the submanifold (dashed box) of the lowest three levels of a transmon circuit. The system exhibits decay from the $|e\rangle$ state to $|g\rangle$ at rate γ_e and is driven by a microwave drive with detuning $\Delta(t)$ and coupling rate J(t). (b) The experimental protocol involves preparing an initial eigenstate $|\pm x\rangle = (|f\rangle \pm |e\rangle)/\sqrt{2}$ using resonant rotation pulses R_{ge}^{π} and $R_{ef,\theta}^{\pi/2}$ (where $\theta=\pi$ or 0, respectively), dynamically tuning the energy operator H(t) for a certain time τ and returning it to its initial value $H(\tau) = H(0)$, followed by post-selective quantum state tomography. (c) By sampling both initial states $|j\rangle \in \{|+x\rangle, |-x\rangle\}$ and postselecting cases where the system does not project onto the ground state, we determine the transition probabilities P_{ij} within the excited-state manifold $\{|e\rangle, |f\rangle\}$.

thereby limiting the dynamics only to the excited-state subspace $\{|e\rangle, |f\rangle\}$, with this no-jump evolution, the role of the spontaneous emission dissipation is now captured by a Hamiltonian term $\frac{-i}{2}L^{\dagger}L = \frac{-i\gamma}{2}|e\rangle\langle e|$ [34,35]. With the addition of a drive that couples the states $|e\rangle$ and $|f\rangle$ with detuning $\Delta(t)$ and rate J(t) [Fig. 2(a)], the evolution of this qubit subspace is described by an effective non-Hermitian Hamiltonian,

$$H_{\text{eff}}(t) = J(t)\sigma_x + \Delta(t)|f\rangle\langle f| + \frac{i\gamma}{4}\sigma_z = H(t) + i\Gamma,$$
 (2)

where $\sigma_x = (|f\rangle\langle e| + |e\rangle\langle f|)$ and $\sigma_z = (|f\rangle\langle f| - |e\rangle\langle e|)$ are Pauli matrices in the excited-state subspace. Here we have also removed an overall loss term proportional to the identity, $(-\frac{i\gamma}{4}\mathbf{1})$, which reflects the exponentially decreasing postselection success. When $\Delta(t) \equiv 0$, the Hamiltonian $H_{\rm eff}(t)$ commutes with the antilinear operator $\mathcal{PT} = \sigma_x \mathcal{K}$, where the parity operator \mathcal{P} is defined as σ_x and the time-reversal operator \mathcal{T} is defined as complex conjugation \mathcal{K} to the Hamiltonian $H_{\rm eff}(t)$, at all times. In the static case, this explicit \mathcal{PT} -symmetry underlies the purely real or purely imaginary eigenvalues $\lambda_{\pm} = \pm \sqrt{J^2 - (\gamma/4)^2}$ of $H_{\rm eff}$ with an exceptional point (EP) degeneracy at $J_{\rm EP} = \gamma/4$.

The transition between real and imaginary eigenvalues of \mathcal{PT} -symmetric systems has been explored extensively in a range of experimental platforms since its introduction by Bender in 1998 [36]. This includes experimental work in optical systems [37–42], ultracold atoms [43], and superconducting qubits [24]. This transition is typically described as a

 \mathcal{PT} -symmetry breaking transition; from unbroken to broken \mathcal{PT} symmetry (real to imaginary eigenvalues) [38]. Notably, the eigenstates of $H_{\rm eff}$ are nonorthogonal near the EP and both the eigenvalues and eigenstates coalesce at the EP. Significant attention has been invested in dynamics in the vicinity of the EP, in particular, where one observes nonreciprocal state transport [44,45], chiral Berry phases [25], and enhanced sensing [46,47]. When $\Delta(t) \neq 0$, the instantaneous eigenvalues $\lambda_{\pm}(t)$ of the non-Hermitian $H_{\rm eff}(t)$ are complex and the Hamiltonian has no explicit \mathcal{PT} symmetry.

In the following, we implement three time-periodic parameter paths,

$$J(t) = \bar{J} + \frac{(J_{\text{max}} - J_{\text{min}})}{2} \cos\left(\frac{2\pi t}{\tau}\right), \quad \Delta(t) = 0, \quad (3)$$

$$\Delta_1(t) = \Delta_{\text{max}} \sin\left(\frac{\pi t}{\tau}\right), \quad J(t) = J_{\text{max}}, \tag{4}$$

$$\Delta_2(t) = \Delta_{\text{max}} \sin\left(\frac{2\pi t}{\tau}\right), \quad J(t) = J_{\text{max}}, \tag{5}$$

where τ is the protocol duration and $\bar{J} = (J_{\text{max}} + J_{\text{min}})/2$.

III. MEASURING WORK DISTRIBUTION

The basis of the experiment is to determine the work distribution P(W) after the system is driven by the cyclic internal energy operator H(t) [Fig. 2(b)]. In our experiment, the TPM procedure consists of three steps: (i) With a sequence of resonant rotations to the transmon circuit, we initialize the system in the eigenstates $|\pm x\rangle = (|f\rangle \pm |e\rangle)/\sqrt{2}$ of the energy operator $H(0) = J_{\text{max}} \sigma_x$. A Gibbs state with inverse temperature β is then synthesized by preparing the two eigenstates with relative probabilities $P_{\pm x} \propto \exp(\mp \beta J_{\text{max}})$. Throughout this paper, we set $\beta = 0.5$ µs/rad, which corresponds to $P_{+x} = 0.98$. (ii) We dynamically apply work to the qubit by tuning the parameters J(t), $\Delta(t)$ as in Eqs. (3)–(5). (iii) We perform a final projective measurement in the basis $\{|g\rangle, |+x\rangle, |-x\rangle\}$ via a single shot, multistate readout of the qutrit, which gives probabilities $\{p_{g,j}, p_{+x,j}, p_{-x,j}\}$ that add up to unity. The TPM protocol determines the total energy change $\Delta U =$ W+Q whose distribution is characterized by the transition probabilities [48]

$$P_{ij}(\tau) = \frac{|\langle i|G(\tau)|j\rangle|^2}{\langle j|G^{\dagger}(\tau)G(\tau)|j\rangle} = \frac{p_{ij}}{p_{+x,i} + p_{-x,i}}, \quad (6)$$

where $i, j = \pm x$ label the eigenstates of the internal energy operator H(0). The work distribution for the non-Hermitian qubit is obtained through the transition probabilities $\{p_{+x,j}, p_{-x,j}\}$ after postselecting on the no-jump evolution. The state-dependent denominator in (6) captures the norm-preserving nature of the postselection process, $\sum_i P_{ij}(\tau) = 1$ [Figs. 2(b) and 2(c)]. For Q = 0, we have $\Delta U = W$ and the exponentiated-work expectation value from (1) is obtained as

$$\langle e^{-\beta W} \rangle(\tau) = \sum_{ij=\pm x} e^{-\beta (J_{\max,i} - J_{\max,j})} P_{ij}(\tau) P_j, \tag{7}$$

where the statistical weights $P_{\pm x} = \{0.98, 0.02\}$ reflect the reservoir temperature, transition probabilities $P_{ij}(\tau)$ are

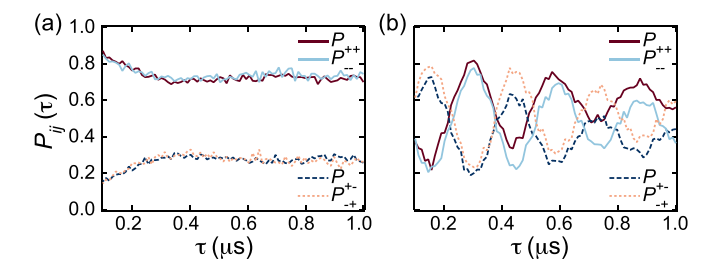


FIG. 3. Symmetries of transition probabilities. (a) Measured probabilities $P_{ij}(\tau)$ for the first path, (3), with $J_{\text{max}} = J_{\text{min}} = 3.74 \, \text{rad/}\mu\text{s}$ are symmetrical under the exchange $+x \leftrightarrow -x$. (b) Measured probabilities for the second path, (4), with the same J_{max} value and $\Delta_{\text{max}} = 10\pi \, \text{rad/}\mu\text{s}$ show clear asymmetry, $P_{++} \neq P_{--}$ and $P_{+-} \neq P_{-+}$. This asymmetry is connected to the absence of \mathcal{PT} symmetry for the Hamiltonian $H_{\text{eff}}(t)$ along the second cyclic path.

experimentally measured for loop duration τ ranging from 0.1 μ s $\leq \tau \leq 1 \mu$ s, $J_{\max,+x} = J_{\max}$, and $J_{\max,-x} = -J_{\max}$.

Figure 3(a) shows that for the first path with zero detuning, Eq. (3), the survival and transition probabilities are equal for the two energy eigenstates. On the contrary, for the second path, Eq. (4) with $\Delta_{\rm max}=10\pi~{\rm rad/\mu s}$, the probabilities $P_{++}\neq P_{--}$ (or, equivalently, $P_{-+}\neq P_{+-}$) are clearly asymmetrical [Fig. 3(b)]. Both cases have $J_{\rm max}=J_{\rm min}=3.74~{\rm rad/\mu s}$. We observe stark differences between these two cases which correspond to Hamiltonians $H_{\rm eff}(t)$ with or without an explicit ${\cal PT}$ symmetry, respectively.

IV. EXPERIMENTAL SETUP

The experimental setup comprises a superconducting circuit that was fabricated and provided by the Superconducting Qubits at Lincoln Laboratory (SQUILL) Foundry at MIT Lincoln Laboratory. The experiments utilize a subportion of a multiqubit chip with relevant components consisting of a tunable transmon qubit with maximum frequency $\omega_{ge}/2\pi =$ 4.373 GHz, dispersively coupled to a readout resonator at coupling rate $g/2\pi = 33$ MHz and linewidth $\kappa/2\pi = 246$ kHz, qubit drive line, and an off-chip coupling line. A solenoid coil fixed to the package allows control of the global flux through the transmon SQUID loop, with bias current filtered at the 4 K stage with a low pass filter (QDevil Q015 QFilter). The qubit is operated at $\omega_{ge}/2\pi=4.25$ GHz and resonator frequency $\omega_r/2\pi = 6.88865$ GHz. To realize the non-Hermiticity, an off-chip coaxial filter is coupled to the qubit to enhance the $|e\rangle$ decay rate to $\gamma_e = 1.57 \ \mu s^{-1}$. The readout signal probes the resonator via a common bus line and is amplified by a Josephson parametric amplifier (BBN-PS2-JPA-DEVICE-QEC) operating with \sim 15 dB of gain.

V. JARZYNSKI EQUALITY AND ITS VIOLATION

Figure 4 summarizes the experimental results for $\langle e^{-\beta W} \rangle(\tau)$ for J(t) variations [(a)–(d)] and $\Delta_1(t)$ variations [(e) and (f)]; each parameter path and the location of the EP is schematically shown in the corresponding panel inset. We see that $\langle e^{-\beta W} \rangle \simeq 1$ for J(t) variations that range from the static case, $J_{\rm max} = J_{\rm min}$ (a), to paths confined to the ${\cal PT}$ -symmetric region, $J_{\rm min} = 0.5 J_{\rm max}$ (b), to paths that traverse across the

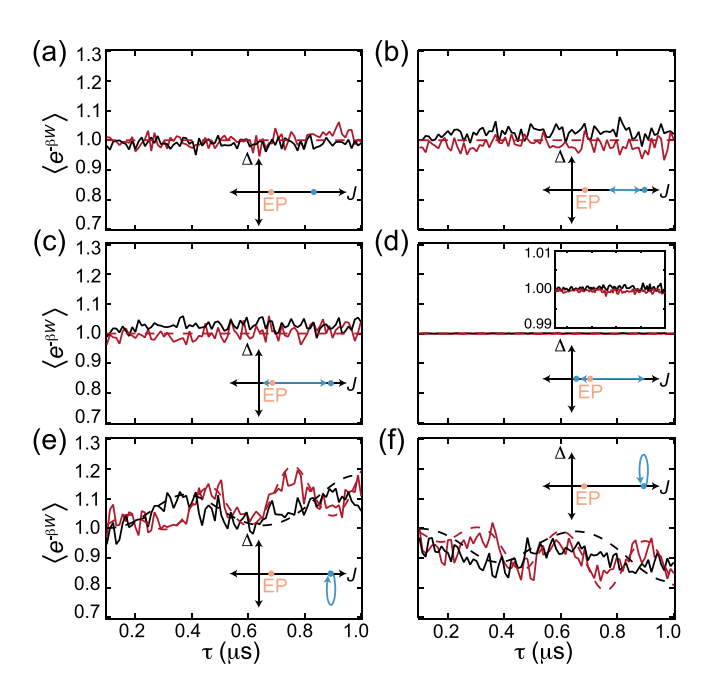


FIG. 4. Jarzynski equality and its violation. Experimental calculation of $\langle e^{-\beta W} \rangle(\tau)$ (solid lines) alongside the simulation results (dashed lines). See Appendix B for simulation details. The insets depict the parameter paths J(t) or $\Delta_1(t)$ and the EP at $J_{\text{EP}} =$ $\gamma/4$. (a)-(d) J(t) sweeps with $J_{\text{max}}=3.74\,\text{rad/}\mu\text{s}$ (red) and $J_{\text{max}}=$ 1.89 rad/ μ s (black). (a) The static case, $J_{\text{max}} = J_{\text{min}}$, satisfies (1). (b) The path going from J_{max} to $J_{\text{min}} = 0.5 J_{\text{max}}$ is in the \mathcal{PT} symmetric region and satisfies (1), as does the path (c) going across the EP to $J_{\min}=0$. (d) For a path starting in the \mathcal{PT} -broken region at $J_{\text{max}} = 0.04 \,\text{rad/}\mu\text{s}$ and reaching across the EP to $J_{\text{min}} > J_{\text{max}}$, the Jarzynski equality (1) holds (upper inset: zoomed-in view of fluctuations). (e), (f) For $\Delta_1(t)$, sweeps with $J_{\text{max}} = 3.74 \,\text{rad/\mu s}$, the average exponentiated-work increasingly deviates from unity: $\Delta_{\rm max} = \mp 10\pi \ {\rm rad/\mu s}$ (red) and $\Delta_{\rm max} = \mp 2\pi \ {\rm rad/\mu s}$ (black). The absence of transition probability symmetry seen in Fig. 3(b) (or a parity-time symmetry) is instrumental to the violation of the Jarzynski equality.

EP into the \mathcal{PT} -broken region with $J_{\min} = 0$ (c). Figure 4(d) shows that starting from the \mathcal{PT} -broken region and traversing across the EP into the \mathcal{PT} -symmetric region also maintains the Jarzynski equality, with much smaller fluctuations arising from the smaller energy scale (upper inset). Thus, the Jarzynski equality is satisfied for arbitrary J(t) sweeps, independent of the real or imaginary nature of eigenvalues of $H_{\rm eff}(t)$ as long as the Hamiltonian has an explicit \mathcal{PT} symmetry. Interestingly, the Jarzynski equality is not expected to be valid for the larger system into which the non-Hermitian qubit is embedded, since the larger system evolves according to a nonunital Lindblad map [49]. For the first path, this explicit PT symmetry also ensures that the corresponding Floquet energy operator H^F has the same energetics as the system's initial energy operator $H(0) = J_{\text{max}}\sigma_x$. In sharp contrast, for one-sided sweeps $\Delta_1(t)$, the average exponentiated work $\langle e^{-\beta W} \rangle(\tau)$ exceeds one for $\Delta_{\text{max}} < 0$ (e) and is below unity for $\Delta_{max} > 0$ (f), thereby indicating that the Jarzynski equality is violated when $H_{\text{eff}}(t)$ or its Floquet counterpart H_{eff}^F do not have an antilinear (parity-time) symmetry.

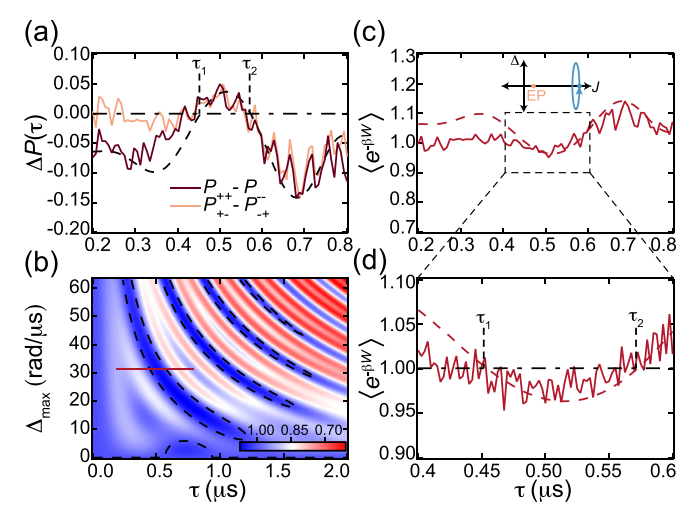


FIG. 5. Emergent parity-time symmetry and Jarzynski equality. For the $\Delta_2(t)$ cyclic path with zero average detuning, the Floquet Hamiltonian always has an emergent \mathcal{PT} symmetry. (a) Yet the transition probability asymmetries $\Delta P(\tau) = P_{++} - P_{--}$ (brown) and $\Delta P(\tau) = P_{+-} - P_{-+}$ (orange) are generally nonzero except at loop times $\tau_1 = 0.455$ µs and $\tau_2 = 0.572$ µs. (b) Simulation of exponentiated-work average (1) while sweeping Δ_{max} and loop time τ . Black dashed contours represent $\langle e^{-\beta W} \rangle = 1$ and correspond to cases where the Floquet energy operator H^F aligns with the initial energy operator H(0). Red solid line: Experimental parameter space. (c) Measured exponentiated-work average for the $\Delta_2(t)$ path with $\Delta_{\text{max}} = 10\pi$ rad/µs (solid line) shows the Jarzynski equality is satisfied at loop times τ_1 , τ_2 . (d) A higher-resolution in loop-time measurement of (c) for τ ranging from 0.4 µs to 0.6 µs. Dashed lines in (a), (c), and (d): simulations

Lastly, we investigate a case where $H_{\text{eff}}(t)$ has no explicit \mathcal{PT} symmetry, and yet its Floquet counterpart H_{eff}^F is parity-time symmetric. In this case, the Jarzynski equality is satisfied only at specific loop times: times where the Floquet energy operator H^F aligns with the system's initial energy operator $H(0) = J_{\text{max}}\sigma_x$. We introduce a different parameter path, Eq. (5), which obeys $\Delta_2(t) = -\Delta_2(\tau - t)$. As a consequence of the zero average detuning, the corresponding Floquet Hamiltonian has an emergent parity-time symmetry, i.e., $H_{\rm eff}^F$ eigenvalues are always real or complex conjugates. Figure 5(a) shows that the measured probability asymmetry $\Delta P(\tau) \equiv P_{++}(\tau) - P_{--}(\tau)$ (brown) or, equivalently, $\Delta P(\tau) = P_{+-}(\tau) - P_{-+}(\tau)$ (orange), is generally nonzero. However, the symmetry under the eigenstate-label exchange $+x \leftrightarrow -x$, indicated by $\Delta P(\tau) = 0$, is recovered at loop times $\tau_1 = 0.455~\mu s$ and $\tau_2 = 0.572~\mu s$. The corresponding simulated exponentiated-work average shows that although generally violated, the Jarzynski equality is satisfied along black dashed contours [Fig. 5(b)]. These contours intersect with the experimentally investigated region at Δ_{max} = $10\pi \text{ rad/}\mu\text{s}$ (red solid line). In general, the experimentally measured $\langle e^{-\beta W} \rangle(\tau)$ is not equal to unity [Fig. 5(c)]. However, at loop times τ_1 and τ_2 , the two equalities $\langle e^{-\beta W} \rangle = 1$ and $\Delta P = 0$ are satisfied simultaneously. A higher-resolution measurement of exponentiated work in a smaller loop-time window shows this effect clearly [Fig. 5(d)].

VI. DISCUSSION AND OUTLOOK

Non-Hermitian Hamiltonians with real spectra [36] realized in open classical systems [38,39,50] have recently materialized in the quantum domain [24,43,51–54]. On top of their role in dynamics, their real eigenvalues are often mistaken for allowed energies of a quantum system [28–33], with implications to thermodynamics. Although the two share conceptual roots, the thermodynamics of non-Hermitian systems remains an open challenge. A consistent formulation of its first law requires distinguishing the Hermitian part H that gives allowed energies [9] from the non-Hermitian Hamiltonian $H_{\rm eff} = H + i\Gamma$ that governs the temporal dynamics. Using the same distinction, we have verified a fluctuation theorem for exponentiated work, i.e., Jarzynski equality (1) for cyclic variations of $H_{\rm eff}(t)$ that include parameter regions with complex eigenvalues.

The Jarzynski equality, rigorously tested in the classical domain [55,56], trivially extends to isolated quantum systems (Q = 0) by equating the work distribution P(W) with the TPM protocol that, technically, generates the distribution $P(\Delta U)$ of internal-energy changes [14]. It also holds in decohering quantum systems [23], but the equality's validity in driven qubits with dissipation, continuous monitoring, or feedback, as tested with the TPM protocol, is disputed [57,58]. In such settings, the tests of the Jarzynski equality require modifications that reflect the energetic cost of information or, equivalently, unique dynamics that encode the monitoring, feedback, and measurement processes [59-64]. Our results show that the coherent qubit dynamics of non-Hermitian Hamiltonians is a class where the Jarzynski equality is preserved when two symmetry considerations are met. First, that the energy basis for the TPM protocol coincides with the Hermitian part of the effective (Floquet or otherwise) Hamiltonian, and second that the non-Hermitian evolution ensures that the qubit has symmetrical amplification or decay rates. Ultimately, violations in the Jarzynski equality are expected to arise from cases where the TPM protocol for characterizing ΔU is contaminated by a nonreversible "classical" heat component. With our symmetry-governed, consistent formulation of the second law of thermodynamics, we anticipate unique opportunities in quantum, nonequilibrium thermodynamics through non-Hermitian models.

ACKNOWLEDGMENTS

We thank A. Auffèves and E. Lutz for helpful comments. This research was supported by NSF Grant No. PHY-1752844 (CAREER), the Air Force Office of Scientific Research (AFOSR) Multidisciplinary University Research Initiative (MURI) Award on Programmable systems with non-Hermitian quantum dynamics (Grant No. FA9550-21-10202), the John Templeton Foundation, Grant No. 61835, ONR Grant No. N00014- 21-1-2630, and the Institute of Materials Science and Engineering at Washington University. Devices were fabricated and provided by the Superconducting Qubits at Lincoln Laboratory (SQUILL) Foundry at MIT Lincoln Laboratory, with funding from the Laboratory for Physical Sciences (LPS) Qubit Collaboratory.

APPENDIX A: ANALYTICAL RESULTS

For a qubit with internal energy operator $H(0) = H(\tau) = J_{\text{max}}\sigma_x$, the exponentiated-work average (7) is given by

$$\langle e^{-\beta W} \rangle = e^{-2\beta J_{\text{max}}} P_{+-}(\tau) P_{-x} + e^{+2\beta J_{\text{max}}} P_{-+}(\tau) P_{+x} + P_{++}(\tau) P_{+x} + P_{--}(\tau) P_{-x}. \tag{A1}$$

It is easy to verify that the right-hand side is equal to unity when the initial density matrix is thermal, i.e., $P_{\pm x} = \exp(\mp \beta J_{\max})/2 \cosh(\beta J_{\max})$, and the transition probabilities are symmetric under the eigenstate-label exchange $+x \leftrightarrow -x$ [Fig. 3(a)]. The exchange-symmetry constraint on the $P_{ij}(\tau)$ holds, provided the elements of the time-evolution matrix $G(\tau)$ satisfy $|G_{++}/G_{-+}| = |G_{--}/G_{+-}|$. By expressing the 2×2 trace-less non-Hermitian Floquet Hamiltonian as $H_{\rm eff}^F = h_x \sigma_x + h_y \sigma_y + h_z \sigma_z$, the exchange-symmetry constraint can be written as

$$\left| \frac{\mathcal{C} - ih_x \mathcal{S}}{(h_y + ih_z) \mathcal{S}} \right| = \left| \frac{\mathcal{C} + ih_x \mathcal{S}}{(h_y - ih_z) \mathcal{S}} \right|,\tag{A2}$$

where $C = \cos(\tau |\mathbf{h}|)$, $|\mathbf{h}| \equiv (h_x^2 + h_y^2 + h_z^2)^{1/2}$, and S = $\sin(\tau |\mathbf{h}|)/|\mathbf{h}|$. The terms \mathcal{C}, \mathcal{S} are real if and only if $|\mathbf{h}|$ is real or purely imaginary. It means the Floquet Hamiltonian H_{eff}^F , with eigenvalues $\pm |\mathbf{h}|$, has an explicit or emergent parity-time (antilinear) symmetry [65]. Equation (A2) further requires that $h_x \in \mathbb{R}$ and h_y , h_z are purely imaginary. Thus, the non-Hermitian, parity-time symmetric, Floquet Hamiltonian $H_{\text{eff}}^F = H^F + i\Gamma^F$ is further constrained to an internal energy operator $H^F = h_x \sigma_x$ that is aligned with the system's initial energy operator H(0). Note that the mere requirement of parity-time symmetry allows for $h_x \in \mathbb{R}$ and a complex $h_y =$ $h_z^* \in \mathbb{C}$. However, in such cases, $H^F = h_x \sigma_x + \operatorname{Re} h_y (\sigma_y + \sigma_z)$ is not aligned with H(0), and the constraint that guarantees exchange symmetry for probabilities, Eq. (A2), is not fulfilled. Thus, Jarzynski equality requires a parity-time symmetric H_{eff}^F with its Floquet energy operator proportional to the system's initial energy operator.

Next, we consider the applicability of the Jarzynski equality to parameter paths that are not closed, i.e., $H(\tau) \neq H(0)$. Figure 6 shows the comparison of $\langle e^{-\beta W} \rangle$ (markers) with the ratio of partition functions $Z(\tau)/Z(0)$ (solid lines) for multiple paths. We observe that when the initial and final energy operators commute with each other, i.e., the energy-basis states are the same, Jarzynski is satisfied. On the other hand, when they do not commute, it is not satisfied. For the non-Hermitian qubit case, this follows by expressing (7) as sums of two orthogonal projectors of H(0) that continue to remain orthogonal after the non-Hermitian evolution. However, a general analytical theory of Jarzynski equality for arbitrary non-Hermitian quantum systems remains an open question.

APPENDIX B: SIMULATIONS

The evolution of the three-level system can be solved using Lindblad equation

$$\frac{\partial \rho_3(t)}{\partial t} = -i[H_c(t), \rho_3(t)] + \sum_{i=1}^4 L_i \rho_3(t) L_i^{\dagger} - \frac{1}{2} \{L_i^{\dagger} L_i, \rho_3(t)\}.$$
(B1)

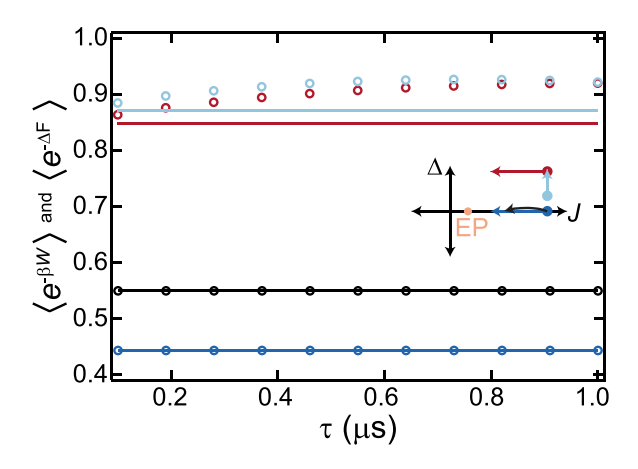


FIG. 6. Simulation of noncyclic paths. Simulation of paths where $Z(0) \neq Z(\tau)$. The markers correspond to the left side of (1) and the solid lines correspond to the computed partition functions from the right-hand side of (1). The dark blue is for a case where the coupling rate J is varied linearly from a maximum of $J_{\text{max}} = 3.74 \ \mu\text{s}^{-1}$ down to $J_{\text{max}}/2$ while $\Delta = 0$. The black case is for the same path but for a quarter period of (3) with $J_{\text{max}} = 3.74 \ \mu\text{s}^{-1}$ and $\Delta = 0$. The red case is the same as the dark blue case but with $\Delta/2\pi = 5 \ \text{MHz}$, breaking the \mathcal{PT} symmetry of the Hamiltonian. The light blue case is for constant $J_{\text{max}} = 3.74 \ \mu\text{s}^{-1}$ and varying $\Delta/2\pi$ linearly from 3 MHz to 5 MHz, thus also breaking the \mathcal{PT} symmetry of the Hamiltonian.

Here $H_c = J(|e\rangle\langle f| + |f\rangle\langle e|) - \Delta/2(|e\rangle\langle e| - |f\rangle\langle f|)$ and the four dissipators L_i include two radiative decay operators $\sqrt{\gamma_e}|g\rangle\langle e|$ and $\sqrt{\gamma_f}|e\rangle\langle f|$, and two dephasing operators

[1] R. Alicki, The quantum open system as a model of the heat engine, J. Phys. A: Math. Gen. 12, L103 (1979). $\sqrt{\gamma_{2e}/2}|e\rangle\langle e|$ and $\sqrt{\gamma_{2f}/2}|f\rangle\langle f|$. The decay and dephasing rates are $\gamma_e = 1.57~\mu s^{-1}$, $\gamma_f = 0.21~\mu s^{-1}$, $\gamma_{2e} = 1.631~\mu s^{-1}$, and $\gamma_{2f} = 0.584~\mu s^{-1}$. Equation (B1) is solved in MATLAB using the Runge-Kutta method to obtain $\rho_3(\tau)$ with suitable initial conditions and thereby calculate each transition probability $P_{ij}(\tau)$. For γ_f , γ_{2e} , $\gamma_{2f} \ll \gamma_e$, the Lindblad results for the $\{|e\rangle, |f\rangle\}$ manifold are identical to those obtained from the non-Hermitian Hamiltonian [48]:

$$\rho_2(\tau) = \frac{G(\tau)\rho_2(0)G^{\dagger}(\tau)}{\text{Tr}[\rho(0)G^{\dagger}(\tau)G(\tau)]}.$$
 (B2)

APPENDIX C: POSTSELECTION AND ERROR ANALYSIS

For the experimental data, we employ postselection by normalizing the state readouts to the population within the $\{|e\rangle,|f\rangle\}$ manifold of states, and the resulting evolution can be described by the non-Hermitian Hamiltonian (2). For each transition probability, we repeat the experiment a total of 8000 times, yet through postselection up to $\sim\!65\%$ of the data is discarded. The statistical (trinomial) error associated with the state readout is typically less than 0.016 for the transition probabilities and less than 0.012 for the exponentiated work. Remnant, point-to-point fluctuations are likely due to residual low-frequency (1/f) fluctuations in the experimental setup. For Figs. 5(a), 5(c), and 5(d), we utilized 24 000 experimental repetitions per point.

^[2] R. Kosloff, A quantum mechanical open system as a model of a heat engine, J. Chem. Phys. **80**, 1625 (1984).

^[3] H. Spohn and J. L. Lebowitz, Irreversible thermodynamics for quantum systems weakly coupled to thermal reservoirs, in *Advances in Chemical Physics* (John Wiley & Sons, Inc., 2007), pp. 109–142.

^[4] J. M. Horowitz, Quantum-trajectory approach to the stochastic thermodynamics of a forced harmonic oscillator, Phys. Rev. E **85**, 031110 (2012).

^[5] J. J. Alonso, E. Lutz, and A. Romito, Thermodynamics of weakly measured quantum systems, Phys. Rev. Lett. 116, 080403 (2016).

^[6] C. Elouard, D. A. Herrera-Martí, M. Clusel, and A. Auffèves, The role of quantum measurement in stochastic thermodynamics, npj Quantum Inf 3, 9 (2017).

^[7] P. M. Harrington, E. J. Mueller, and K. W. Murch, Engineered dissipation for quantum information science, Nat. Rev. Phys. 4, 660 (2022).

^[8] D. A. Lidar, Lecture notes on the theory of open quantum systems, arXiv:1902.00967.

^[9] M. Naghiloo, D. Tan, P. M. Harrington, J. J. Alonso, E. Lutz, A. Romito, and K. W. Murch, Heat and work along individual trajectories of a quantum bit, Phys. Rev. Lett. 124, 110604 (2020).

^[10] C. Jarzynski, Nonequilibrium equality for free energy differences, Phys. Rev. Lett. 78, 2690 (1997).

^[11] J. Kurchan, Fluctuation theorem for stochastic dynamics, J. Phys. A: Math. Gen. 31, 3719 (1998).

^[12] G. E. Crooks, Entropy production fluctuation theorem and the nonequilibrium work relation for free energy differences, Phys. Rev. E **60**, 2721 (1999).

^[13] H. Tasaki, Jarzynski relations for quantum systems and some applications, arXiv:cond-mat/0009244.

^[14] G. Huber, F. Schmidt-Kaler, S. Deffner, and E. Lutz, Employing trapped cold ions to verify the quantum Jarzynski equality, Phys. Rev. Lett. **101**, 070403 (2008).

^[15] J. Kurchan, A quantum fluctuation theorem, arXiv:condmat/0007360.

^[16] S. Mukamel, Quantum extension of the Jarzynski relation: Analogy with stochastic dephasing, Phys. Rev. Lett. 90, 170604 (2003).

^[17] T. Albash, D. A. Lidar, M. Marvian, and P. Zanardi, Fluctuation theorems for quantum processes, Phys. Rev. E 88, 032146 (2013).

^[18] A. E. Rastegin, Non-equilibrium equalities with unital quantum channels, J. Stat. Mech.: Theory Exp. (2013) P06016.

^[19] T. B. Batalhão, A. M. Souza, L. Mazzola, R. Auccaise, R. S. Sarthour, I. S. Oliveira, J. Goold, G. D. Chiara, M. Paternostro, and R. M. Serra, Experimental reconstruction of work distribution and study of fluctuation relations in a closed quantum system, Phys. Rev. Lett. 113, 140601 (2014).

^[20] S. An, J.-N. Zhang, M. Um, D. Lv, Y. Lu, J. Zhang, Z.-Q. Yin, H. T. Quan, and K. Kim, Experimental test of the quantum Jarzynski equality with a trapped-ion system, Nat. Phys. 11, 193 (2015).

- [21] F. Cerisola, Y. Margalit, S. Machluf, A. J. Roncaglia, J. P. Paz, and R. Folman, Using a quantum work meter to test non-equilibrium fluctuation theorems, Nat. Commun. 8, 1241 (2017).
- [22] T. P. Xiong, L. L. Yan, F. Zhou, K. Rehan, D. F. Liang, L. Chen, W. L. Yang, Z. H. Ma, M. Feng, and V. Vedral, Experimental verification of a Jarzynski-related information-theoretic equality by a single trapped ion, Phys. Rev. Lett. 120, 010601 (2018).
- [23] A. Smith, Y. Lu, S. An, X. Zhang, J.-N. Zhang, Z. Gong, H. T. Quan, C. Jarzynski, and K. Kim, Verification of the quantum nonequilibrium work relation in the presence of decoherence, New J. Phys. 20, 013008 (2018).
- [24] M. Naghiloo, M. Abbasi, Y. N. Joglekar, and K. W. Murch, Quantum state tomography across the exceptional point in a single dissipative qubit, Nat. Phys. 15, 1232 (2019).
- [25] M. Abbasi, W. Chen, M. Naghiloo, Y. N. Joglekar, and K. W. Murch, Topological quantum state control through exceptional-point proximity, Phys. Rev. Lett. 128, 160401 (2022).
- [26] D. C. Brody and E.-M. Graefe, Mixed-state evolution in the presence of gain and loss, Phys. Rev. Lett. 109, 230405 (2012).
- [27] Z. Bian, L. Xiao, K. Wang, F. A. Onanga, F. Ruzicka, W. Yi, Y. N. Joglekar, and P. Xue, Quantum information dynamics in a high-dimensional parity-time-symmetric system, Phys. Rev. A 102, 030201(R) (2020).
- [28] S. Deffner and A. Saxena, Jarzynski equality in \mathcal{PT} -symmetric quantum mechanics, Phys. Rev. Lett. **114**, 150601 (2015).
- [29] B. Gardas, S. Deffner, and A. Saxena, Non-Hermitian quantum thermodynamics, Sci. Rep. 6, 23408 (2016).
- [30] M. Zeng and E. H. Yong, Crooks fluctuation theorem in \mathcal{PT} -symmetric quantum mechanics, J. Phys. Commun. 1, 031001 (2017).
- [31] B.-B. Wei, Quantum work relations and response theory in parity-time-symmetric quantum systems, Phys. Rev. E 97, 012114 (2018).
- [32] B.-B. Wei, Links between dissipation and Rényi divergences in PT-symmetric quantum mechanics, Phys. Rev. A 97, 012105 (2018).
- [33] Z.-Y. Zhou, Z.-L. Xiang, J. Q. You, and F. Nori, Work statistics in non-Hermitian evolutions with Hermitian endpoints, Phys. Rev. E **104**, 034107 (2021).
- [34] K. Mølmer, Y. Castin, and J. Dalibard, Monte Carlo wavefunction method in quantum optics, J. Opt. Soc. Am. B **10**, 524 (1993).
- [35] J. Dalibard, Y. Castin, and K. Mølmer, Wave-function approach to dissipative processes in quantum optics, Phys. Rev. Lett. 68, 580 (1992).
- [36] C. M. Bender and S. Boettcher, Real spectra in non-Hermitian Hamiltonians having PT symmetry, Phys. Rev. Lett. 80, 5243 (1998).
- [37] B. Peng, Ş. K. Özdemir, F. Lei, F. Monifi, M. Gianfreda, G. L. Long, S. Fan, F. Nori, C. M. Bender, and L. Yang, Parity-time-symmetric whispering-gallery microcavities, Nat. Phys. 10, 394 (2014).
- [38] Ş. K. Özdemir, S. Rotter, F. Nori, and L. Yang, Parity-time symmetry and exceptional points in photonics, Nat. Mater. 18, 783 (2019).
- [39] A. Guo, G. J. Salamo, D. Duchesne, R. Morandotti, M. Volatier-Ravat, V. Aimez, G. A. Siviloglou, and D. N. Christodoulides, Observation of PT-symmetry breaking in complex optical potentials, Phys. Rev. Lett. 103, 093902 (2009).

- [40] C. E. Rüter, K. G. Makris, R. El-Ganainy, D. N. Christodoulides, M. Segev, and D. Kip, Observation of parity-time symmetry in optics, Nat. Phys. 6, 192 (2010).
- [41] H. Hodaei, M.-A. Miri, M. Heinrich, D. N. Christodoulides, and M. Khajavikhan, Parity-time-symmetric microring lasers, Science **346**, 975 (2014).
- [42] L. Xiao, X. Zhan, Z. H. Bian, K. K. Wang, X. Zhang, X. P. Wang, J. Li, K. Mochizuki, D. Kim, N. Kawakami, W. Yi, H. Obuse, B. C. Sanders, and P. Xue, Observation of topological edge states in parity-time-symmetric quantum walks, Nat. Phys. 13, 1117 (2017).
- [43] J. Li, A. K. Harter, J. Liu, L. de Melo, Y. N. Joglekar, and L. Luo, Observation of parity-time symmetry breaking transitions in a dissipative Floquet system of ultracold atoms, Nat. Commun. 10, 855 (2019).
- [44] H. Xu, D. Mason, L. Jiang, and J. G. E. Harris, Topological energy transfer in an optomechanical system with exceptional points, Nature (London) 537, 80 (2016).
- [45] W. Liu, Y. Wu, C.-K. Duan, X. Rong, and J. Du, Dynamically encircling an exceptional point in a real quantum system, Phys. Rev. Lett. 126, 170506 (2021).
- [46] H. Hodaei, A. U. Hassan, S. Wittek, H. Garcia-Gracia, R. El-Ganainy, D. N. Christodoulides, and M. Khajavikhan, Enhanced sensitivity at higher-order exceptional points, Nature (London) 548, 187 (2017).
- [47] W. Chen, Ş. K. Özdemir, G. Zhao, J. Wiersig, and L. Yang, Exceptional points enhance sensing in an optical microcavity, Nature (London) 548, 192 (2017).
- [48] A. V. Varma, J. E. Muldoon, S. Paul, Y. N. Joglekar, and S. Das, Extreme violation of the Leggett-Garg inequality in nonunitary dynamics with complex energies, Phys. Rev. A 108, 032202 (2023).
- [49] A. E. Rastegin and K. Życzkowski, Jarzynski equality for quantum stochastic maps, Phys. Rev. E 89, 012127 (2014).
- [50] M.-A. Miri and A. Alù, Exceptional points in optics and photonics, Science 363, eaar7709 (2019).
- [51] F. Klauck, L. Teuber, M. Ornigotti, M. Heinrich, S. Scheel, and A. Szameit, Observation of PT-symmetric quantum interference, Nat. Photonics 13, 883 (2019).
- [52] Y. Wu, W. Liu, J. Geng, X. Song, X. Ye, C.-K. Duan, X. Rong, and J. Du, Observation of parity-time symmetry breaking in a single-spin system, Science **364**, 878 (2019).
- [53] L. Ding, K. Shi, Q. Zhang, D. Shen, X. Zhang, and W. Zhang, Experimental determination of \mathcal{PT} -symmetric exceptional points in a single trapped ion, Phys. Rev. Lett. **126**, 083604 (2021).
- [54] N. Maraviglia, P. Yard, R. Wakefield, J. Carolan, C. Sparrow, L. Chakhmakhchyan, C. Harrold, T. Hashimoto, N. Matsuda, A. K. Harter, Y. N. Joglekar, and A. Laing, Photonic quantum simulations of coupled *PT*-symmetric Hamiltonians, Phys. Rev. Res. 4, 013051 (2022).
- [55] J. Liphardt, S. Dumont, S. B. Smith, I. Tinoco, and C. Bustamante, Equilibrium information from nonequilibrium measurements in an experimental test of Jarzynski's equality, Science 296, 1832 (2002).
- [56] O.-P. Saira, Y. Yoon, T. Tanttu, M. Möttönen, D. V. Averin, and J. P. Pekola, Test of the Jarzynski and Crooks fluctuation relations in an electronic system, Phys. Rev. Lett. 109, 180601 (2012).

- [57] F. W. J. Hekking and J. P. Pekola, Quantum jump approach for work and dissipation in a two-level system, Phys. Rev. Lett. 111, 093602 (2013).
- [58] J. P. Pekola, Y. Masuyama, Y. Nakamura, J. Bergli, and Y. M. Galperin, Dephasing and dissipation in qubit thermodynamics, Phys. Rev. E **91**, 062109 (2015).
- [59] S. Toyabe, T. Sagawa, M. Ueda, E. Muneyuki, and M. Sano, Experimental demonstration of information-to-energy conversion and validation of the generalized Jarzynski equality, Nat. Phys. 6, 988 (2010).
- [60] Z. Gong, Y. Ashida, and M. Ueda, Quantum-trajectory thermodynamics with discrete feedback control, Phys. Rev. A 94, 012107 (2016).
- [61] Y. Masuyama, K. Funo, Y. Murashita, A. Noguchi,
 S. Kono, Y. Tabuchi, R. Yamazaki, M. Ueda, and
 Y. Nakamura, Information-to-work conversion by

- Maxwell's demon in a superconducting circuit quantum electrodynamical system, Nat. Commun. 9, 1291 (2018).
- [62] M. Naghiloo, J. J. Alonso, A. Romito, E. Lutz, and K. W. Murch, Information gain and loss for a quantum Maxwell's demon, Phys. Rev. Lett. 121, 030604 (2018).
- [63] X. Song, M. Naghiloo, and K. Murch, Quantum process inference for a single-qubit Maxwell demon, Phys. Rev. A 104, 022211 (2021).
- [64] X. Linpeng, L. Bresque, M. Maffei, A. N. Jordan, A. Auffèves, and K. W. Murch, Energetic cost of measurements using quantum, coherent, and thermal light, Phys. Rev. Lett. 128, 220506 (2022).
- [65] A. K. Harter and Y. N. Joglekar, Connecting active and passive PT-symmetric Floquet modulation models, Prog. Theor. Exp. Phys. 2020, 12A106 (2020).